A MULTI-CHANNEL COOLING SYSTEM FOR MULTIPLE HEAT SOURCE

by

Shanglong XU**, *Weijie WANG, Zongkun GUO, Xinglong HU, and Wei GUO

Department of Mechatronics Engineering, University of Electronic Science and Technology of China, Chengdu, China

Original scientific paper
DOI: 10.2298/TSCI140313123X

High-power electronic devices with multiple heating elements often require temperature uniformity and operating within their functional temperature range for optimal performance. A multi-channel cooling experiment apparatus is developed for studying heat removal inside an electronic device with multiple heat sources. It mainly consists of a computer-controlled pump, a multi-channel heat sink for multi-zone cooling, and the apparatus for measuring the temperature and pressure drop. The experimental results show the system and the designed multi-channel heat sink structure can control temperature distribution of electronic device with multiple heat sources by altering coolant flow rate.

Key words: *multiple heat sources, microchannel heat sink, cooling system*

Introduction

Intelligence, integration and miniaturization has become the main development trend of modern electronic equipment in the few decades [1-3]. The system-level, device-level, and chip-level power electronic components usually have several heat elements, such as computer cabin [4, 5]. It is important on thermal design of all the heat elements to ensure that the temperatures in them are maintained within their functional temperature range [6]. Microchannel cooling has received a great deal of attention and been used to cool heat-generating electronic device, because of its simple structure and good cooling capacity [7, 8]. Heat transfer in rectangular microchannels of different geometry parameters was investigated by Lee *et al.* [9] and Zhang *et al.* [10]. Some laws and correlations in ducts of large dimension are also applicable to the microchannels [11].

The multi-cooling channels can be used to cool these electronic components with different powers and temperatures [12]. Dede and Liu [13] investigated a multi-pass branching microchannel heat sink cooling one heat source. But multiple heat sources widely exist in various mechanical and electronic equipment, and it is not easy to properly cool them and uneven cooling will cause unexpected performance responses. For some applications, this temperature uniformity can be critical to device effectiveness [14]. Thus, it is necessary to develop an experimental apparatus to study thermal performance of electronic device with multiple heat sources and design methodology for the multi-cooling channel heat sink.

* Corresponding author; e-mail: xusl1607@gmail.com

Turkakar and Okotucu-Ozyurt [15] studied dimensional optimization of silicon microchannel heat sinks is performed by minimizing the total thermal resistance. The study has been performed for localized multiple heat sources. Tounsi *et al.* [16] proposed an adaptive multiple cooling surfaces compact thermal model and boundary condition independent multiple heat sources to study the thermal performance of power components. Mao *et al.* [17] established a compact thermal model for microchannel with high temperature uniformity subjected to multiple heat sources.

Cho *et al.* [18] conducted an experimental study on microchannel heat sinks about flow distribution with non-uniform heat flux conditions. Thermal load is applied to the microchannel heat sinks by nine separate heaters in order to provide uniform or non-uniform heat flux, including local heating at hotspots.

Kim *et al.* [19] investigated thermal management of liquid-cooled cold plates for multiple heat sources. The experimental apparatus consisted of a constant-temperature bath, a DC power supply, a cooling water circulation pump, temperature measuring devices, and data acquisition unit. Six cold plates were made for cooling multiple heat sources inside a humanoid robot.

These researches focused on improvement of thermal performance for multi-channel heat sinks by theoretic and experimental study. The report on the development of special experiment apparatus and manifold multi-channels for multiple heat sources cooling is also important for further electronic cooling technology. In this study, an experiment system for managing and cooling multiple heat sources is developed to study the thermal performances of the two multi-channel heat sink structures. The cold plate with four microchannel regions made of copper for cooling four heat sources is fabricated and connected each other by a channel circulation. The pressure drop and thermal performance in two different multiple cold plates are compared and analyzed in terms of flow rate and surface temperature for four microchannel regions.

Cooling system and multi-channel heat sinks

A novel experiment system is established to study thermal performances of multiple heat-generating components with different powers. It mainly consists of a computer-controlled pump, a computer, a heating device with four separate heating blocks, a microchannel heat sink for multi-zone cooling, and the apparatuses for measuring the temperature and pressure drop. A schematic diagram of the experimental flow loop is shown in fig. 1.

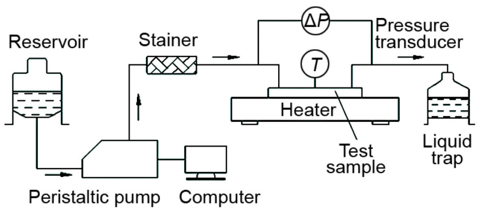

Figure 1. Schematic diagram of the experimental flow loop

Heating blocks

The intelligent temperature controller was chosen to provide heat source. Four heating blocks of 30 mm × 30 mm × 30 mm are made of aluminum to simulate four heat generating components (fig. 2). Four wire heaters installed into the heating blocks are controlled separately by four DC power supplies. The average temperature of each block is controlled by adjusting voltage on the power supply and displayed on Nixie tubes. They generate multi-heat sources and can supply different temperatures for different blocks. There is no heat transfer between different blocks. But the temperature is uniform within the same block. We can set the required temperature value of each heating block. If the temperature sensor in heating-generating device notices that the aimed temperature has been reached, it will make the heating coil stop heating. Heat from the heater is also estimated from the input voltage and current. The micro-channel heat sink is attached to the heating block closely. The thermal compound is used to attach them to reduce thermal contact. Then, the heat sink and the heating block are carefully insulated by glass fiber and asbestos to reduce heat loss to the ambient.

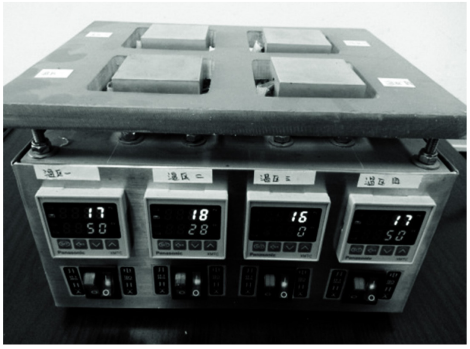

Figure 2. Heat-generating device with four heating blocks

Microchannel heat sink

Microchannel should be designed with respect to a major design target, which may be the less pumping power or the uniform distribution of temperature [16]. The designed two micro-channel cold plates and its major dimension is shown in fig. 3 and made of copper material. The interconnected four microchannel regions are attached to four heating blocks, respectively. The designed cooling capacity of the four microchannel regions is different because their channel numbers and distance between two adjacent channels are not same. Each channel region is 37.5 mm × 40.0 mm area. The depth of all channels is 1 mm. The cover part of total test region is 200 mm × 200 mm area with 1.0 mm in height and the inlet/outlet tubes of 5.0 mm in outer diameter. The thickness of heat sink base which is contacted to the heating block is 1 mm. To prevent the leakage of the cooling water, the cover and the base are adhered using epoxy adhesive. The total heights of heat sinks are 3.2 mm. The microchannel cold plates fabricated by laser engraving are shown in

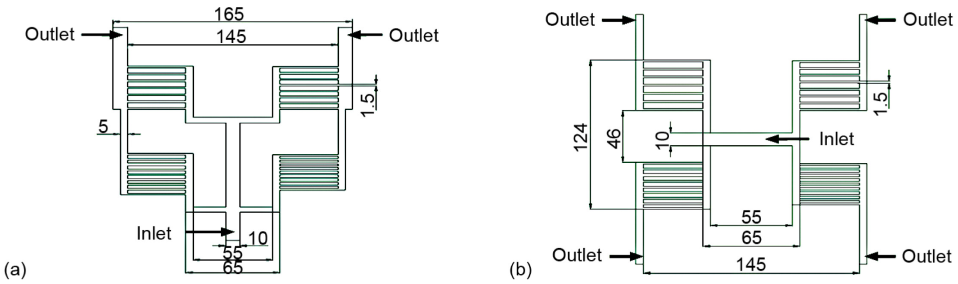

Figure 3. Designed structure and dimension of two microchannel heat sinks [mm]

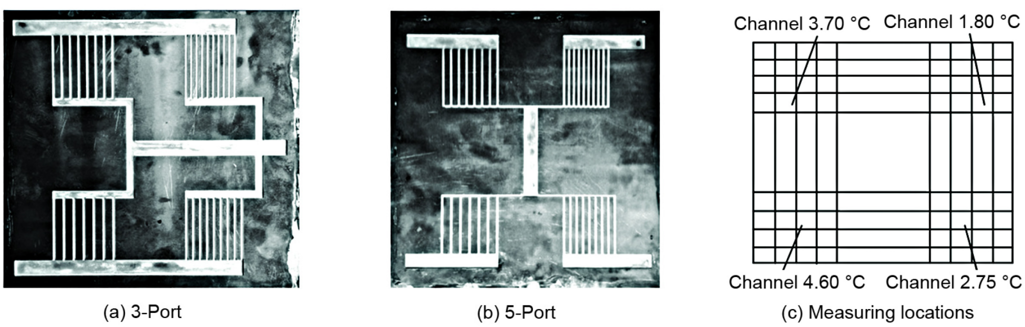

Figure 4. Fabricated microchannel cold plates and measuring locations in cold plate cover; (a) 3-port, (b) 5-port, and (c) measuring locations

figs. 4(a) and (b). To obtain the temperatures related to multichannels and heat blocks, the four channel regions in the heat sink are divided into 16 subregions. The total subregions are 64 in the measuring surface, as shown in fig. 4(c). Each small square is a measurement point.

Measure device

The temperature acquisition is Fluke type infrared thermometer (IRT) that is suitable for non-contact temperature measurement. This optical device can measure radiation energy, reflect energy and transmitted energy on the detector, and covert the signal to a digital readout on the display. Its measuring range is from 0 °C to 450 °C. The accuracy and display resolution are ±0.5 °C and 0.1 °C, respectively, which can satisfy the test requirements document. The system calibration is conducted by comparing its measurements with the values by a T-type thermocouple to reduce error from surface emissivity. We can get the surface temperature distribution of the heat sink. Differential pressure transducer (JYD-KO-BAD) is used to measure pressure drop in microchannel heat sink. The CH6 CONTRONIX digital display instrument is selected as the pressure drop collector, whose model number is CH6/A-HRTB1. The measurement error of the pressure transducers is 0. 25%.

Pump and computer

In this system, the selected cooling water circulation pump is BT/L series of intelligent peristaltic pump BT300L, which is controlled by the computer. The pump speed is controlled by a computer programmed digital speed controller. The water flow rate supplied to the system can be regulated by software developed in our lab in the computer and is used as feedback to the computer with an interface to the digital speed controller. The flow rate is also shown in digital display instrument of the pump. The range of rotate speed is 0.1-350 rounds per minute. The outer and inner diameters of tube used in it are 5 mm and 3 mm, respectively. The largest measurement uncertainty of the pump transducers is approximately 0.5%. The error of volumetric flow rate is less than 0.5%.

Experimental procedure

The microchannel cold plate including subdomain number is attached on four heat sources. The flow circulation is composed as shown in fig. 1. Experimental conditions are shown in tab. 1. A cartridge heater embedded into an aluminum block generates uniform heat and is controlled by DC power supply. The heating of block is controlled by adjusting voltage on the power supply and can provide 500 W maximum power. The error of each surface temperature is controlled to keep within ±1 °C. A cold plate with the circulation pump is used to supply constant-temperature cooling water to cold plates. The flow rates of cooling water are 400, 500, 600, 700, 800, and 900 ml per minute, respectively, and are controlled by adjusting voltage or the software in the computer. The inlet temperature of cooling water is 20 °C. The working fluid flows successively through the tube and connector, filter, and microchannel heat sink and finally is collected to a container. The measuring locations on the cover surface by IRT are shown in fig. 4(c).

Table 1. Fluid flow and heat transfer parameters in the experiment

T_{in} [°C]	T_0 [°C]	Q [ml per minute]
20	80, 75, 70, 60	400-900

Numerical simulation

A numerical simulation is used to verify the experimental results. The numerical simulation is performed using FLUENT 13.0 based on the finite volume method to compare with the experimental results. The conservation equations of mass, momentum, and energy are solved. The parameters is same with that in the experiment. The solid region of the heat sink is copper with the thermal conductivity of k_s = 387 W/mK. The coolant is water, with density 1000 kg/m^3, dynamic viscosity $8.55\cdot10^{-4}$ kg/ms, specific heat 4179 J/kgK, and thermal conductivity 0.613 W/mK.

The local Reynolds numbers of fluid in the channels, Re = $\rho VD/\mu$ (where ρ is the water density, V – the flow speed, D – the hydrodynamic diameter, and μ – the dynamic viscosity), are different when the flow rates of cooling water are from 400 to 900 ml per minute. The maximum of local Reynolds number occurs at the inlet of heat sink where the flow velocity is highest. The different volumetric flow corresponding to inlet Reynolds numbers is 2200-5000 in 3-port heat sink. But in 5-port heat sink, it is 1100-2500. When the Reynolds number is larger than 1800, the turbulent model is used. Otherwise the model of laminar flow is used. The following assumptions are made in modeling the heat transfer in microchannel heat sink to simplify the analysis: (1) steady-state, (2) incompressible fluid, (3) constant coolant properties (20-65 °C), and (4) negligible viscous dissipation.

Non-uniform temperatures are applied to the four microchannel bottom surfaces of the heat sink to generate initial heat flux. Computational girds for both solid and fluid regions are generated using orthogonal hex-map scheme. The model is meshed by an adaptive gridding meshing method. A total of 704626 grid points are assigned to the entire computational domain. Fine grids are located at the fluid flow region. A mesh sensitivity study is performed by changing the number of the grid cells to validate the accuracy of the simulation results. When the total number of grid points used increases from 704626 to 1401255, and 2122325, the change of the maximum temperature is less than 1.8%. Then, the problems are solved with the minimum reduction in normalized residuals for each variable at less than $1.0\cdot10^{-5}$.

Results and discussion

The designed system supplies multi-heat sources and different flow rates controlled by computer. The multi-channel network can cool the heat generating components with different initial temperatures. The multi-channel heat sink contains four regions with different channel number and distance between two adjacent channels. The flow resistance is different while the coolant flows through the four regions. It is small in the region where

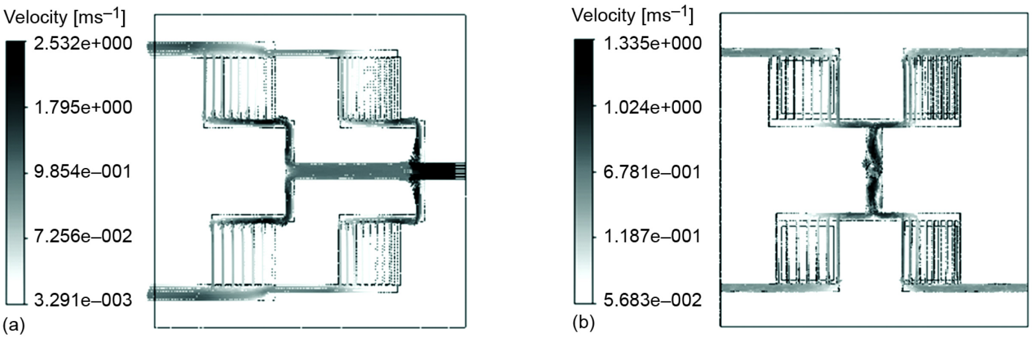

Figure 5. Velocity distribution among the microchannels at 800 ml flow rate in 3-port (a) and 5-port (b)

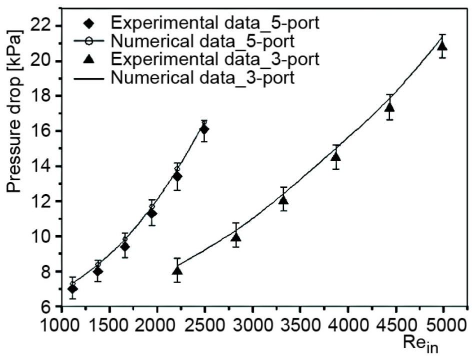

Figure 6. Experimental and numerical pressure drops in 3-port and 5-port multichannel configuration at different inlet Reynolds numbers

there are more channel numbers although the inlet flow rate is same. The distribution of flow rate in the channels is similar although the inlet flow rate is different. Figure 5 shows the numerical results of the velocity distribution among the microchannels at 800 ml flow rate in 3-port and

5-port. The flow rate in the four interconnected multi-channel regions is different as the channel number is different. The maximum velocity occurs in a rectangular groove of the inlet. Although the inlet velocity of 3-port is almost twice of 5-port, the 5-port heat sink has a more uniform velocity and flow rate distribution than the 3-port heat sink in the four sub-regions.

The pressure drop characteristics are as important as the thermodynamic performance in the selection of a viable compact heat exchanger. The comparison of the pressure drops obtained experimentally with those obtained numerically for the two multi-channel heat sinks at different inlet Reynolds numbers is shown in fig. 6. The repeatability of the approach is validated by retesting some experimental conditions and the error bars are plotted. The numerical results follow the same patterns and agree well with the experimental data. In the two heat sinks, the pressure drop becomes higher as the inlet Reynolds number increases. The pressure drops in 5-port microchannel configuration are smaller than in 3-port microchannel at the same inlet flow rate due to lower flow velocity in the individual channel and reduced average coolant path resulting in maximal mass flow.

Figures 7 and 8 show the surface temperature distribution of the experiment and simulation in the two heat sinks at the flow rate of 800 ml per minute. The temperature values of measured locations in the multi-channel heat sink are shown in fig. 4(c). The maximum and local temperatures are different in 3-port and 5-port channel networks including four cooling regions. The measured maximum, minimum, and average temperatures in 3-port structure are approximately 56.0 °C, 44.5 °C, and 51.0 °C, respectively, which is 20% higher than that in the 5-port structure. So the temperature difference is about 9 °C between them. Figures 7 and 8 also show that the temperature distributions in the four heating regions are more uniform for the different cooling channel number and space. The difference of average temperature in the four channel regions is about 3-8 °C although the initial temperature difference supplied by four heat sources is 15 °C. The wall temperatures of the two heat sinks attached to four heat sources are in the range of 38~55 °C at the flow rate of 800 ml per minute. We can obtain ex-

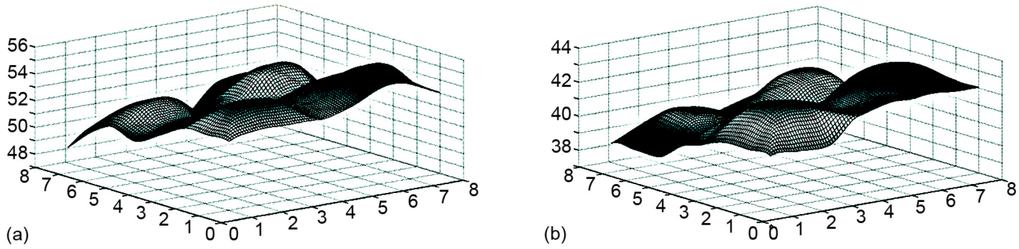

Figure 7. Temperature distribution of the upper wall by experiment (a) 3-port multichannel, (b) 5-port multichannel

pected temperature distribution by altering the local structure configuration of the microchannel network according to thermal design requirement of multiple heat source devices.

The average temperatures decrease sharply in the four cooling regions of the microchannel heat sink. For the region in which initial temperature is highest, the maximum and

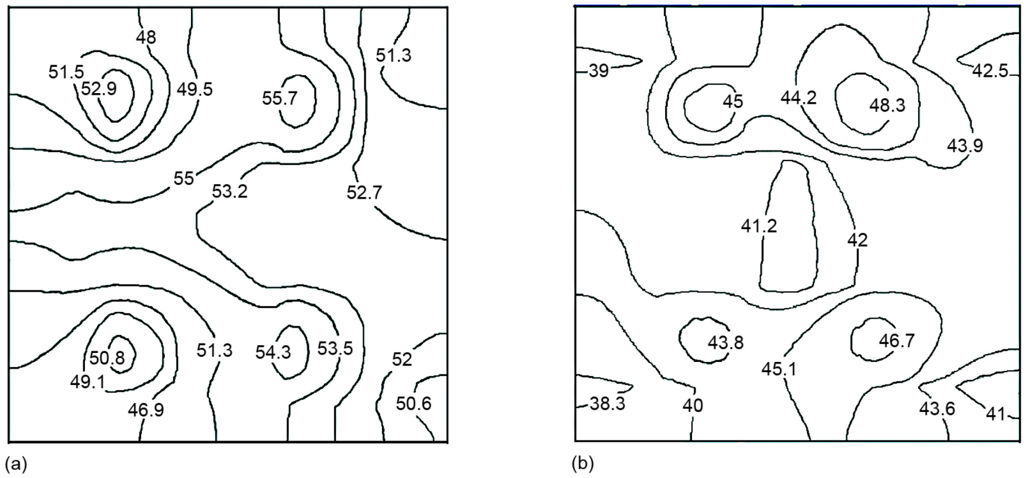

Figure 8. Temperature distribution of the upper wall by simulation (a) 3-port multichannel, (b) 5-port multichannel

average temperatures are slightly higher than other regions. The temperature distribution in the whole multichannel heat sink is more uniform than the initial non-uniform temperature condition generated by the four heat blocks. Junction temperature deviation of the heat sources is approximately 7 °C. In fig. 9, the average temperatures for each hot region condition in the two heat sinks are compared.

The experimental and numerical results of the temperature drops in the two multichannel heat sinks at different inlet Reynolds numbers are shown in fig. 10. Similar to the change of the pressure drop, the temperature decreases monotonically with the increase of the inlet Reynolds number. The total temperature drops are approximately 19 °C and 36 °C with

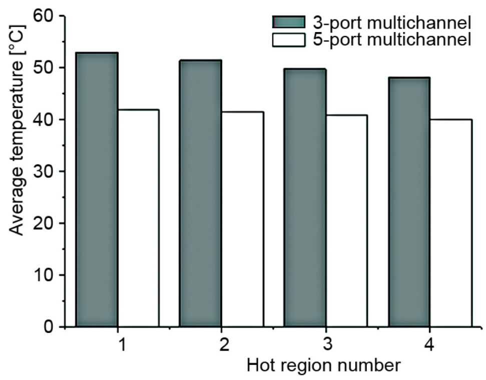

Figure 9. Average temperatures in four multichannel regions

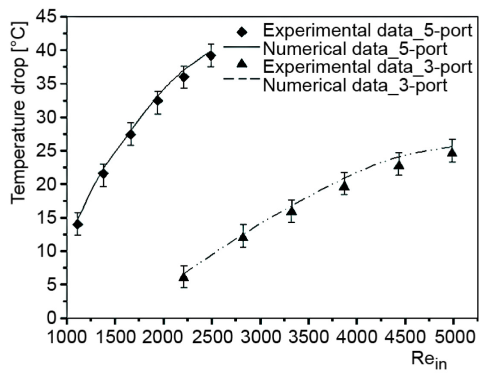

Figure 10. Experimental and numerical temperature drops in 3-port and 5-port multichannel configuration at different inlet Reynolds numbers

3-port and 5-port heat transfer structures which corresponds to a 400 ml per minute volumetric flow rate. When the flow rate is higher, the two heat sinks have a better thermal performance and a more uniform distribution of temperature. In general, the temperature differences in 5-port microchannel structure are from 14 °C to 40 °C, while they are from 6 °C to 26 °C in 3-port structure at coolant flow rate of 400~900 ml per minute. It also suggests the different heat dissipation efficiencies of the two heat sinks at a given volume flow rate of water. The 5-port structure has a higher efficiency than the 3-port, which is attributed to the heat enhancement of working fluid flowing through the channel system.

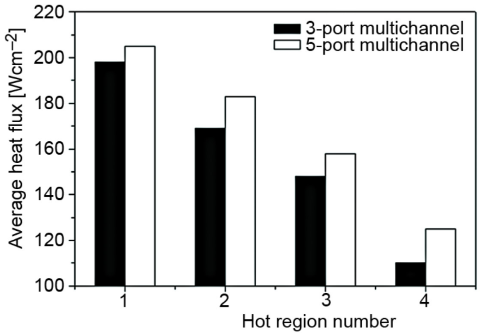

Figure 11. Average heat flux in the location applied four heat resources

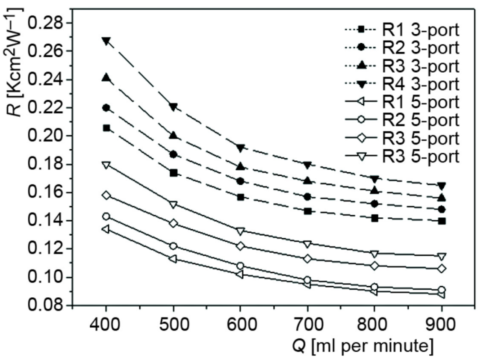

Figure 12. Local thermal resistance and volumetric flow rate for the two heat sinks

The heat flux distributions in the two microchannel heat sinks are also obtained. The average heat flux in location approached the heating surface by simulation is shown in the fig. 11. While heat flux is the independent variable in the study, the same initial heat flux through two samples with different microchannels will lead to different temperature rise within the microchannels and different heat flux distribution on the samples. The initial heat fluxes applied in the four regions are 242 W/cm^2, 195 W/cm^2, 172 W/cm^2, and 145 W/cm^2, respectively. When the sample is cooled by 3-port and 5-port multichannels, all the heat fluxes in the two samples decline. The maximum heat fluxes in the two samples are respectively 223 W/cm^2 and 212 W/cm^2 and the average in the four surfaces are in the range of 110~205 W/cm^2, at the inlet flow rate of 800 ml per minute. The corresponding fluid temperature differences between the inlet and outlet of the 3-port and 5-port networks are approximately 25 °C and 35 °C, respectively.

The heat transfer performance of microchannel heat sink is characterized by the thermal resistance. It is defined by:

$$R_{\text{total}} = \frac{T_{\text{heater}} - T_{\text{in}}}{q} \tag{1}$$

where T_{heater} is the maximum temperature of wall, T_{in} – the bulk temperature of inlet fluid, and q – the heat flux of heat source.

The relationship between the local thermal resistance and volumetric flow rate for the two heat sinks is shown in fig. 12. R_1, R_2, R_3, and R_4 are the location thermal resistances for each channel region of heat sink, respectively. For each heat sink, the thermal resistance decreases with the increase of flow rate, from 0.27 to 0.14 Kcm^2/W and 0.18 to 0.09 Kcm^2/W, respectively. The thermal resistance of 3-port heat sink is generally higher than that of 5-port heat sink. In the four regions, the increase of the flow rate reduces all local thermal resistances. For the two heat sinks, further increasing the flow rate to 800 ml per minute, the overall thermal resistance begins a slow decline.

Conclusions

The intelligent control cooling system and the thermal characteristics of two multi-channel cold plates to cool multiple heat sources are studied as well as local temperature pressure drop, and thermal resistance in the four temperature regions. The designed system is an effective cooling apparatus for the power component with multiple heat sources and an experimental instrument for studying the non-uniform heat flux condition and structure design of microchannel heat sink.

A major design target for microchannel is the less pumping power and the uniform distribution of temperature as well as a low peak temperature, especially for a non-uniform initial heat flux or temperature condition. This study supplies the microchannel design and performance assessment and tries extending them to take into account the most general cases including multiple heat sources and multi-channel cooling conditions.

Acknowledgment

This work was supported by National Natural Science Foundation of China (No. 51176025) and the Fundamental Research Funds for the Central Universities (ZYGX 2012J102).

Nomenclature

k_s – thermal conductivity, [$Wm^{-1}K^{-1}$]
Q – flow rate, [$mlmin^{-1}$]
q – heat flux, [Wcm^{-2}]
Re – Reynolds number
R_{total} – thermal resistance, [Kcm^2W^{-1}]
T_0 – heating source temperature, [°C]
T_{heater} – maximum temperature of wall, [°C]
T_{in} – inlet temperature, [°C]

Greek symbols

μ – dynamic viscosity, [$kgm^{-1}s^{-1}$]
ρ – water density, [kgm^{-3}]

References

[1] Mudawar, I., Assessment of High-Heat-Flux Thermal Management Schemes, *IEEE, Components and Packaging Technologies, 24* (2001), 2, pp. 122-141
[2] Dede, E. M., Optimization and Design of a Multipass Branching Microchannel Heat Sink for Electronics Cooling, *Journal of Electronic Packaging, 134* (2012), 12, pp. 1-10
[3] Dang, T. J., Teng, T., Comparisons of the Heat Transfer and Pressure Drop of the Microchannel and Minichannel Heat Exchangers, *Heat and Mass Transfer, 47* (2011), 10, pp. 1311-1322
[4] Anandakrishnan M., CFD Simulations of Thermal and Flow Fields inside a Desktop Personal Computer Cabin with Muti-Core Processors, *Engineering Applications of Computational Fluid Mechanics, 3* (2009), 2, pp. 277-288
[5] Hemanth, B. N., Balai, C., Application of ACFD Approach to a System Level Thermal Simulation, *International Journal of Heat and Technology, 25* (2007), 1, pp. 43-48
[6] Hetsroni, G., *et al.,* Nonuniform Temperature Distribution in Electronic Devices Cooled by Flow in Parallel Microchannels, *IEEE Tran, Compon. Packag. Tech., 24* (2001), 1, pp. 16-23
[7] Solovitz, S. A., Mainka, J., Manifold Design for Micro-Channel Cooling with Uniform Flow Distribution, *ASME Journal of Fluids Engineering, 133* (2011), 5, ID 051103
[8] Xu, S. L., *et al.*, The Design of an Asymmetric Bionic Branching Channel for Electronic Chips Cooling, *Heat and Mass Transfer, 49* (2013), 6, pp. 827-834
[9] Lee, P.-S., *et al.*, Investigation of Heat Transfer in Rectangular Microchannels, *Int. J. Heat Mass Transfer, 48* (2005), 9, pp. 1688-1704
[10] Zhang, J., *et al.*, An Experimental Study of the Characteristics of Fluid Flow and Heat Transfer in the Multiport Microchannel Flat Tube, *Applied Thermal Engineering, 65* (2014), 1, pp. 209-218
[11] Mokrani, O., *et al.*, Fluid Flow and Convective Heat Transfer in Flat Microchannels, *Int. J. Heat Mass Transfer, 52* (2009), 5, pp. 1337-1352
[12] Monier-Vinard, E., *et al.,* Analytical Thermal Modelling of Multilayered Active Embedded Chips into High Density Electronic Board, *Thermal Science, 17* (2013), 3, pp. 695-706

[13] Dede, E. M., Liu, Y., Experimental and Numerical Investigation of a Multi-Pass Branching Microchannel Heat Sink, *Applied Thermal Engineering, 55* (2013), 1, pp. 51-60
[14] Habra, W., *et al*., Transient Compact Modeling for Multi Chips Components, *Proceedings,* 11th International Workshop on THERMINIC, Belgirate, Italy, 2005, pp. 28-30
[15] Turkakar, G., Okutucu-Ozyurt, T., Dimensional Optimization of Microchannel Heat Sinks with Multiple Heat Sources, *International Journal of Thermal Sciences, 62* (2012), Dec., pp. 85-92
[16] Tounsi, P., *et al*., Adaptive Multiple Cooling Surfaces Compact Thermal Model (CTM), and Boundary Condition Independent Multiple Heat Sources CTM, *Proceedings*, 25th IEEE SEMI-THERM Symposium, Washington, Cal., USA, 2009, pp. 232-238
[17] Mao, Z, *et al.*, Compact Thermal Model for Microchannel Substrate with High Temperature Uniformity Subjected to Multiple Heat Sources, *Proceedings*, 61th Electronic Components and Technology Conf., San Diego , USA, 2011, pp. 1663-1672
[18] Cho, E. S., *et al.*, Experimental Study on Microchannel Heat Sinks Considering Mass Flow Distribution with Non-Uniform Heat Flux Conditions, *International Journal of Heat and Mass Transfer, 53* (2010), 9, pp. 2159-2168
[19] Kim, S. Y., *et al*., Thermal Management of Liquid-Cooled Cold Plates for Multiple Heat Sources in a Humanoid Robot, *Proceedings*, 4th Assembly and Circuits Technology Conf., Beijing, China, 2009, pp. 453-456

Paper submitted: March 3, 2014
Paper revised: October 18, 2014
Paper accepted: November 1, 2014